REGRESSION-BASED UNMIXING OF URBAN LAND COVER

FELIPE CAMACHO HURTADO

SALZBURG UNIVERSITY

ADVANCED REMOTE SENSING

SALZBURG, AUSTRIA

NOVEMBER 21, 2022

CONTENTS

1. Objectives

- Provide an insight into different band statistics associated with Hyperspectral Imagery.
- Describe the reflectance behaviors for various land coverages.
- Understand how the “Regression-based Unmixing” approach is applied with EnMAP.
- Quantitative and Qualitative compare the fraction maps resulting from the “*Regression-based Unmixing*” approach.

2. Used Software

- QGIS 3.26.3 – Buenos Aires.
- EnMAP – Box 3 (3.11.0)

3. Used Data

Data Type	Filename	Description
Raster	Hymap_berlin.bsq	Airborne hyperspectral data from the HyMap sensor with a spatial resolution of 3.6m, 111 bands and 346x3200 pixels (ENVI Standard Band Sequential bsq)
Raster	Enmap_berlin.bsq	Spaceborne hyperspectral data from the EnMAP sensor (here simulated from HyMAP) with a spatial resolution of 30m, 177 bands and 220x400 pixels (ENVI Standard Band Sequential bsq)
Vector	landcover_berlin_point.gpkg	Detailed land cover reference information categorized in a hierarchical class scheme.

Table 1. Data used for the project. (EnMap)

4. Procedures

For this project, three main processes were carried out and their results discussed. First, for the hyperspectral image “*Enmap_berlin.bsq*”, based on the Raster Statistics obtained using the “*Band Statistics*” tool in EnMAP, several questions regarding its spectral bands/ranges were answered.

Secondly, a spectral library was created using impervious, low vegetation, tree, soil, and water coverages for the hyperspectral image “Enmap_berlin.bsq”. For this procedure, the reflectance behaviors were discussed.

Finally, the “Regression-Based-Unmixing” tool was ran in QGIS with the EnMAP plugin, which generated five fraction maps. For this procedure, the performance of each class on it’s respectively fraction map was qualitative and quantitative analyzed.

1. <u>Raster Statistics Calculation</u>

    a. Step-By-Step

In **EnMap-Box 3 (3.11.0)**, clicked on Tools > Band Statistics 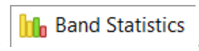

, and selected the "enmap_berlin.bsq" layers as the Raster layer parameter. Then, clicked on "All Bands 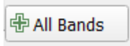

.

    b. How many spectral bands does the "*enmap_berlin.bsq*" hyperspectral image contain?

Based on the documentation (Check "*Used Data*" section), the "*enmap_berlin.bsq*" image should have 177 bands. After checking the resulting band statistics (Figure 1), this number of bands were confirmed.

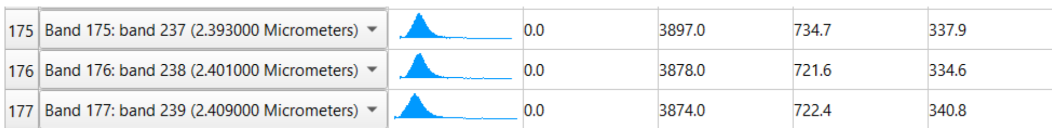

175	Band 175: band 237 (2.393000 Micrometers)		0.0	3897.0	734.7	337.9
176	Band 176: band 238 (2.401000 Micrometers)		0.0	3878.0	721.6	334.6
177	Band 177: band 239 (2.409000 Micrometers)		0.0	3874.0	722.4	340.8

Figure 1. Last 3 spectral bands for the "enmap_berlin.bsq" image.

    c. What is the spectral range of the provided hyperspectral image?

The spectral range for the "*enmap_berlin.bsq*" image, goes from 0.46 Micrometers up to 2.409 Micrometers. (Figure 2).

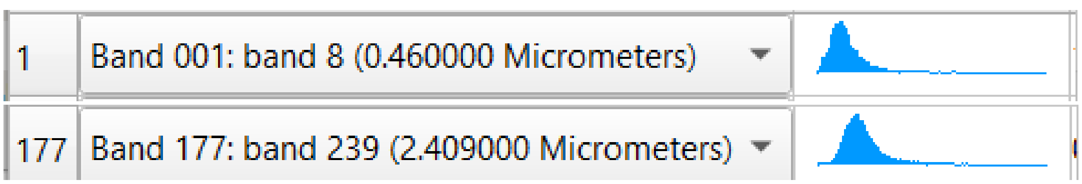

Figure 2. First and last spectral band for the "enmap_berlin.bsq" image.

2. <u>Spectral Signatures Creation</u>

    a. Step-By-Step

In **EnMap-Box 3 (3.11.0)**, clicked on "Open a spectral library window" 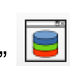, then activated the "Identify pixel profiles and show them in a Spectral Library" tool  and clicked (on the "*enmap_berlin.bsq"* image) on the pixels corresponding to the desired feature whose spectral profile would like to be created. Finally, after each spectral profile was created, clicked on "Add profiles" 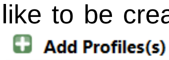

, to store the related spectral profile.

The process described above, was performed twice for the water, soil, tree, low vegetation and impervious classes. The "Hymap_berlin.bsq" image was used as visual reference to create the samples. Check below each collected sample.

Figure 3. *Water class, first sample.*

Figure 4. *Water class, second sample.*

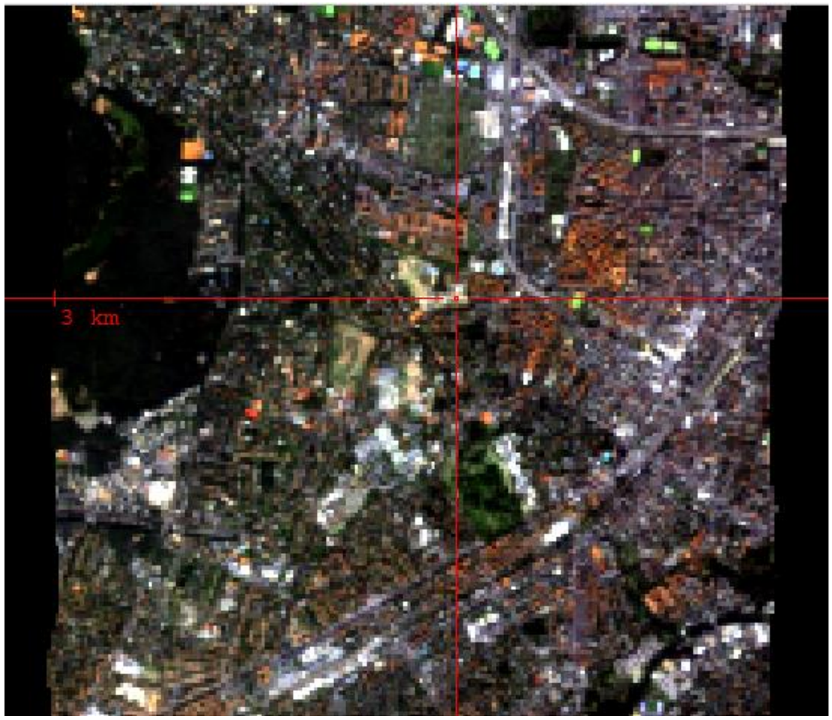

Figure 5. *Soil class, first sample.*

Figure 6. Soil class, second sample.

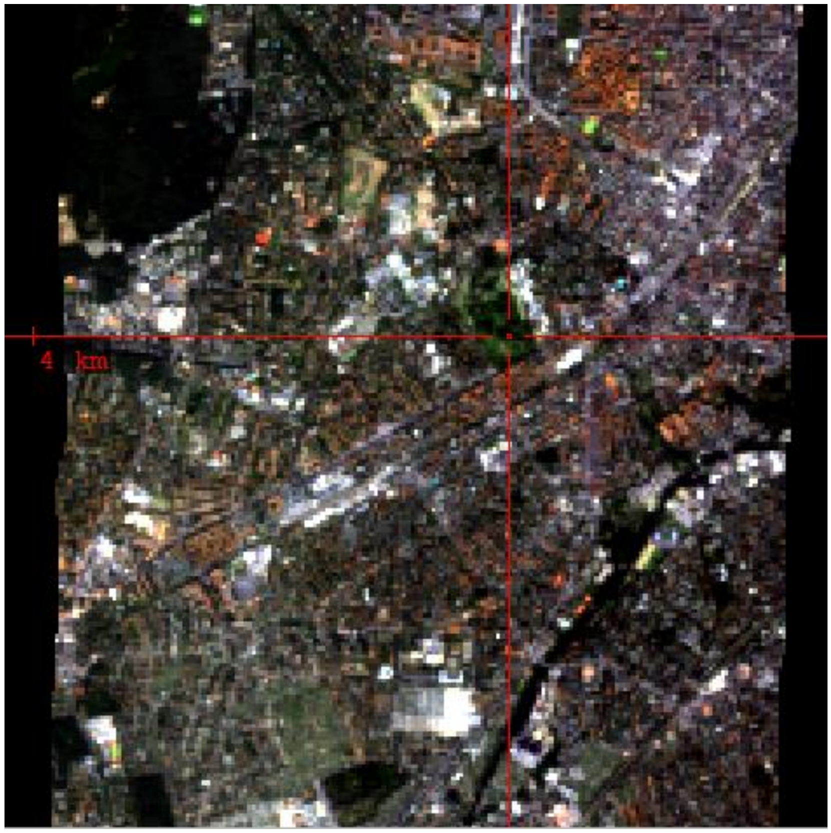

Figure 7. Tree *class, first sample.*

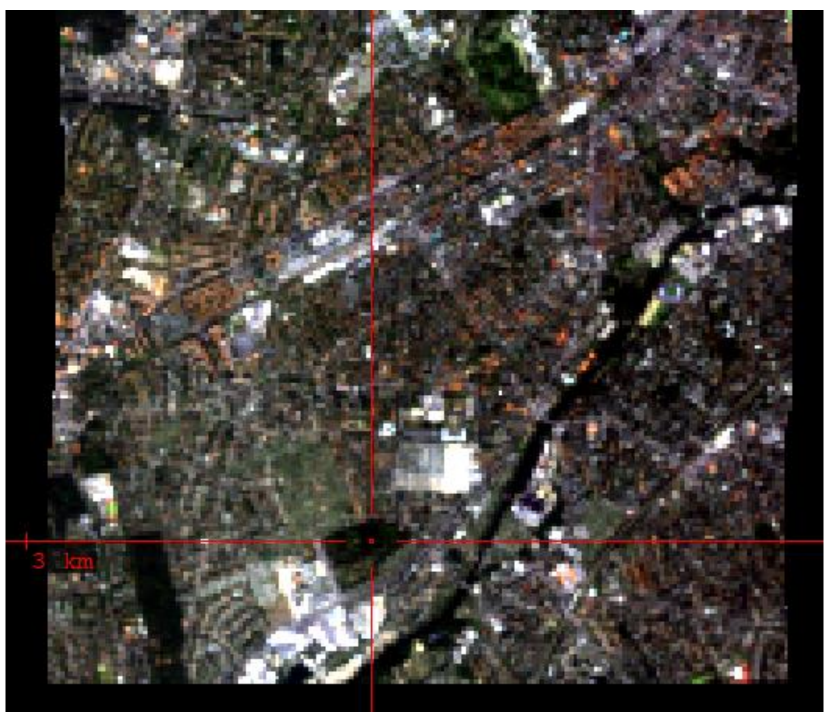

Figure 8. Tree class, second sample.

Figure 9. Low vegetation class, first sample.

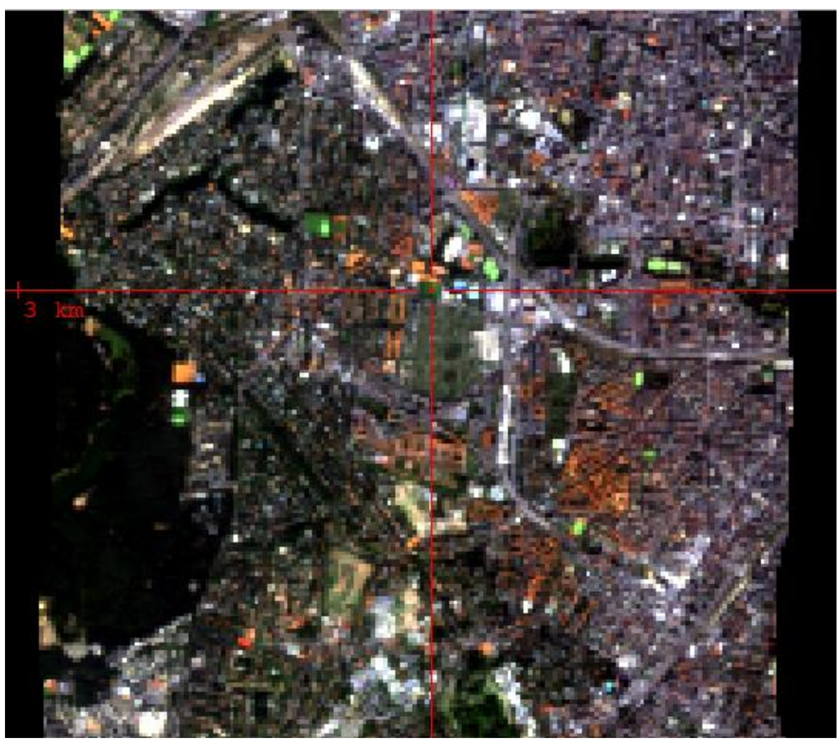

Figure 10. Low vegetation class, second sample.

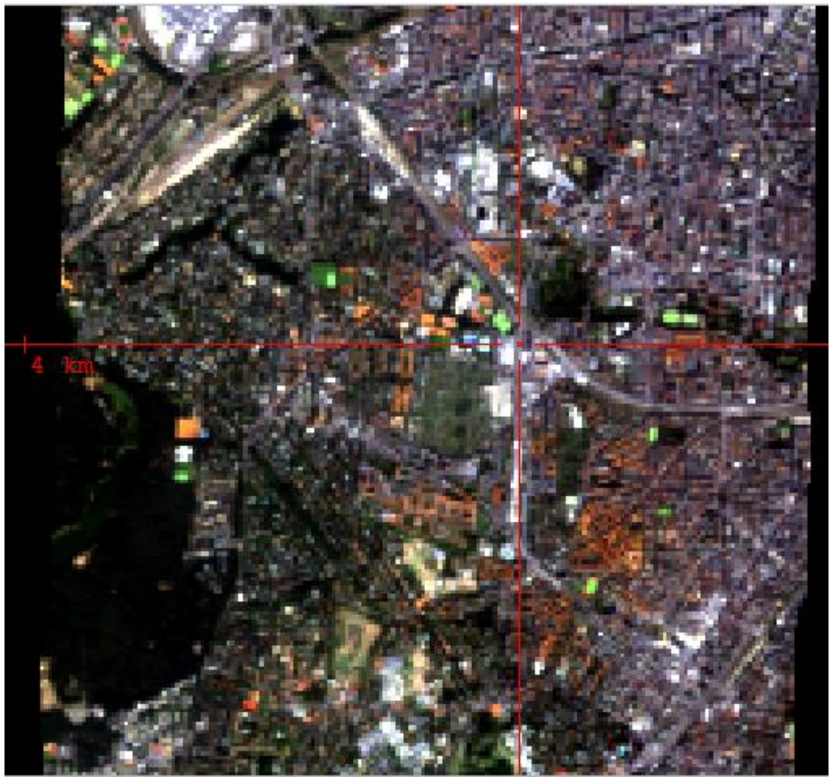

Figure 11. Impervious class, first sample.

Figure 12. Impervious class, second sample.

b. Results

Based on the samples above, the spectral library (Figure 13) was created. In the figure below, the spectral ranges are between 0.0 and 2.4 μm.

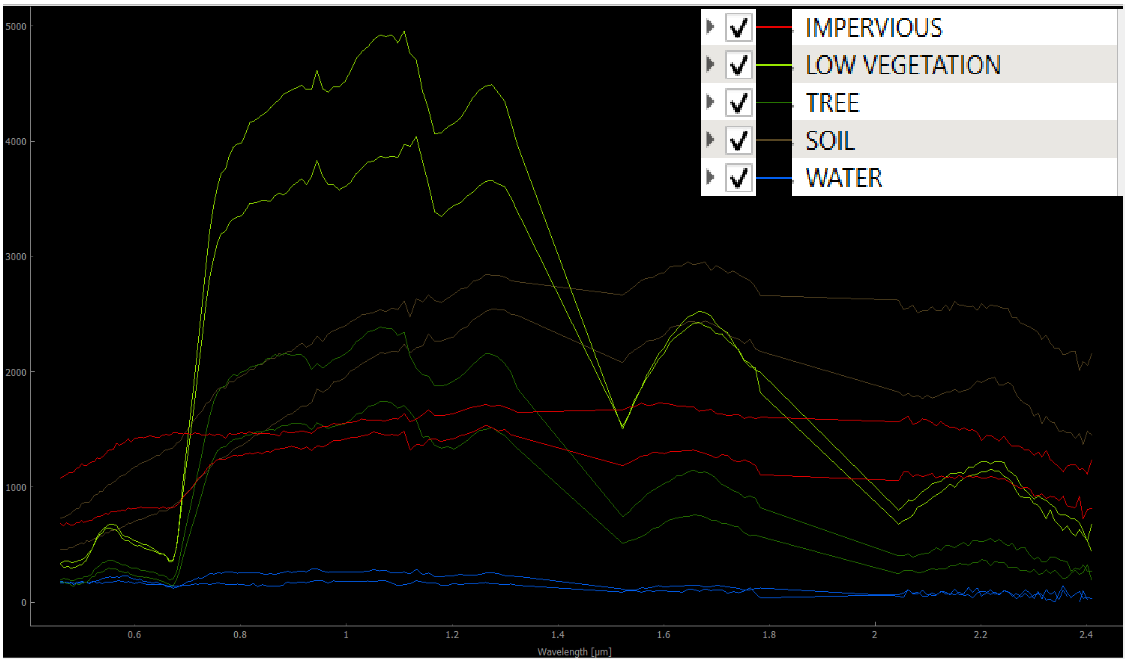

Figure 13. Resulting Spectral Library.

For the Tree and Low Vegetation classes, the spectral signatures showed a low reflectance value in the visible portion of the electromagnetic spectrum. However, there is a small peak near the 0.5 µm wavelength, which corresponds to the green band. The highest reflectance for both classes can be evidenced starting at 0.8 µm wavelength, which corresponds to the start of the Infrared electromagnetic portion. In this case, it can be observed that one of the Low vegetation samples has less reflectance in the NIR band, which can be related to less healthy vegetation.

For the water classes, low reflectance values can be evidenced along the spectral range shown, which it's explained by the high radiant flux absorption for water bodies. Additionally, a small peak can be observed in the NIR range.

Regarding the Impervious classes, even though the reflectance values are higher when compared to the water classes, they are still consistently low across the spectral range.

Finally, for the soil classes, it was observed that the higher reflectance values are after the NIR band. Additionally, there is a dip in the range at 1.3 µm and 1.50 µm, which can be related to water absorption and the presence of soil moisture.

3. <u>Regression-Based-Unmixing Application</u>

   a. Step-By-Step

In **EnMap-Box 3 (3.11.0)**, to perform "Regression-Based-Unmixing", the first step is to click on "Applications" > Regression-Based Unmixing. Then, click on "Create classification dataset" (from categorized vector layer and feature raster). The resulting tool has to be configured using the landcover points, the hyperspectral map, and additional parameters shown in figure 14. Click on run.

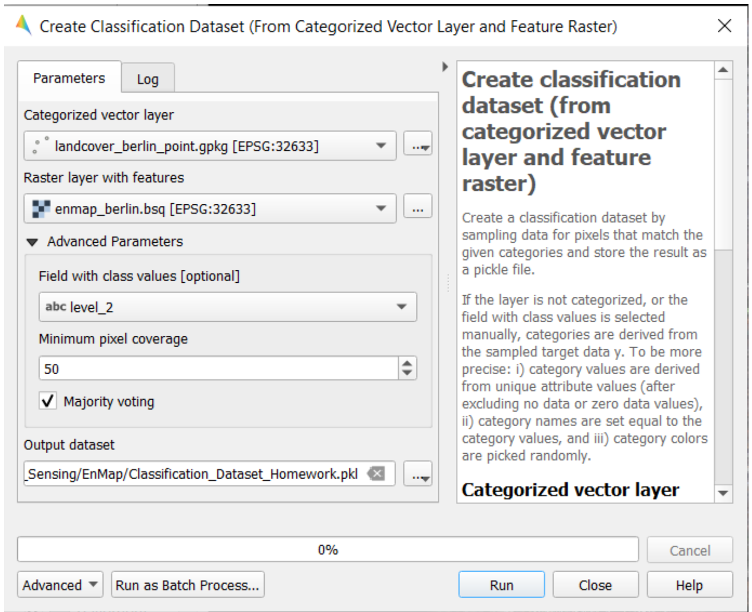

Figure 14. *“*Create classification dataset” tool configuration.

Then, the resulting Classification Dataset was used as a parameter for the “Endmember dataset” for the “Regression-Based Unmixing” tool. In this case, the **LinearRegression** was selected as Regressor. After setting up the additional parameters (Figure 15), select a location where to create the class fraction layer and the classification layer, and click run.

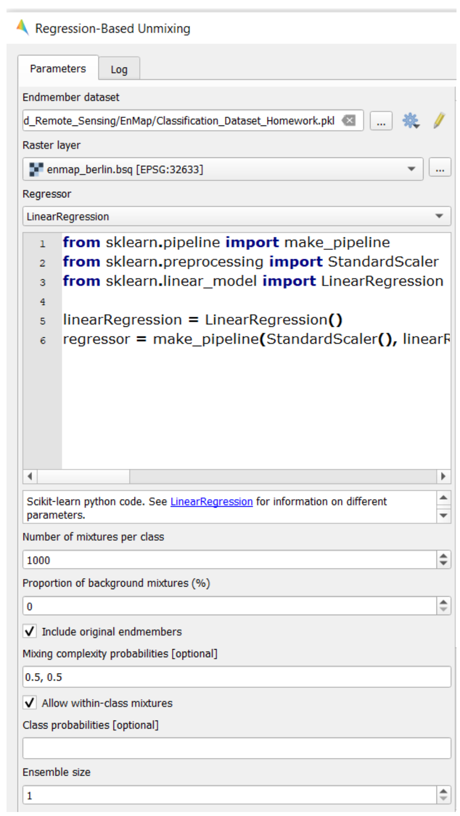

Figure 15. *“*Regression-Based Unmixing” tool configuration.

After running the “Regression-Based Unmixing” tool, the outputs were a classification map, and a fractional map in which each band corresponds to a sample class. In the next section, the band statistics for the fractional map will be briefly discussed, in addition to quantitative analysis of each band in the fractional map, based on the fractional values for two sample pixels per band.

b. Results

For the fractional map, it was observed that the minimum and maximum range (Figure 16) included negative and positive (higher than one) values. In this case, the sum of fractions per pixel for all the classes may be often larger than 1, but its physically meaningful range will be between 0 and 1 (EnMap).

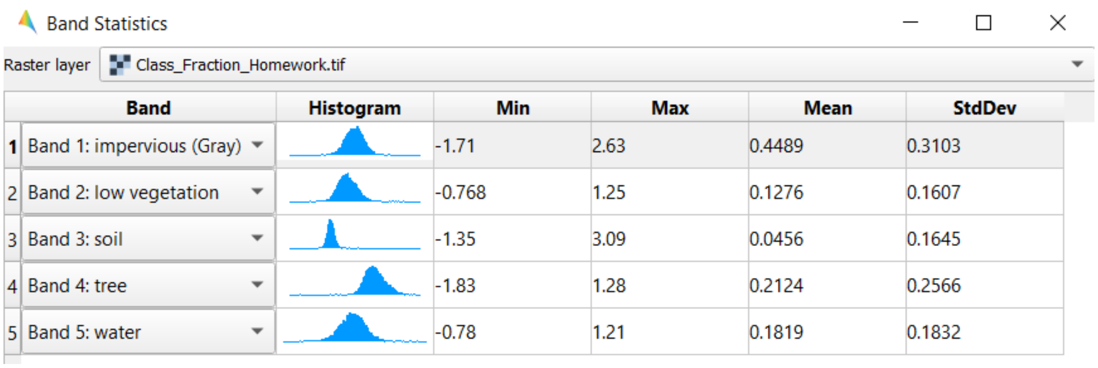
Band Statistics

Raster layer: Class_Fraction_Homework.tif

	Band	Histogram	Min	Max	Mean	StdDev
1	Band 1: impervious (Gray)		-1.71	2.63	0.4489	0.3103
2	Band 2: low vegetation		-0.768	1.25	0.1276	0.1607
3	Band 3: soil		-1.35	3.09	0.0456	0.1645
4	Band 4: tree		-1.83	1.28	0.2124	0.2566
5	Band 5: water		-0.78	1.21	0.1819	0.1832

Figure 16. Band statistics for the Fractional Map.

Water Fractional Band (5)

For the Water class (Figure 17), water bodies like lakes and rivers were effectively differentiated. The fractional values confirmed the above for both sample pixels (Figure 18 – 19), as water abundance was between 0.84 and 0.91. Additionally, the impervious class was overestimated, as it was the second predominant class in the sampling pixel, with values of 0.25 and 0.29.

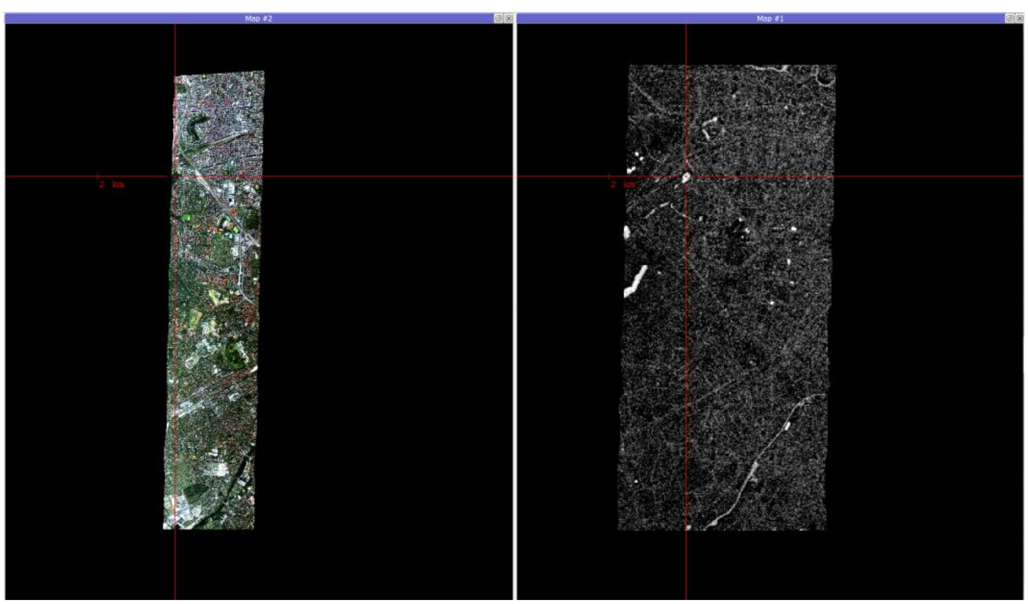

Figure 17. Water Class - Fractional Map.

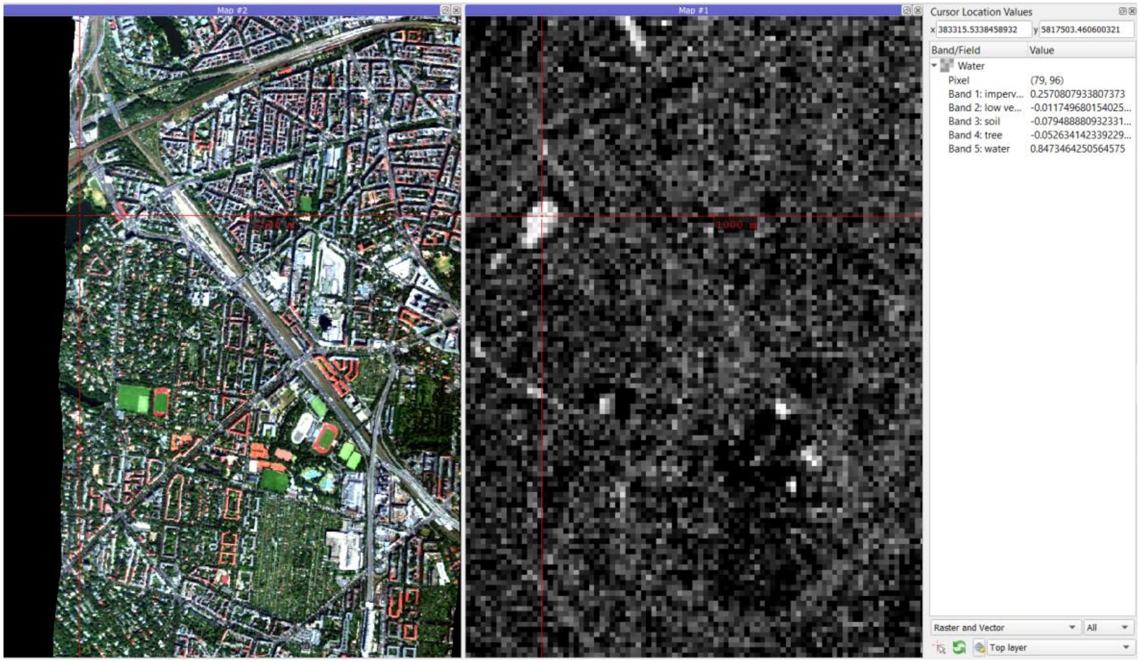

Figure 18. Water Class – Sample Pixel 1.

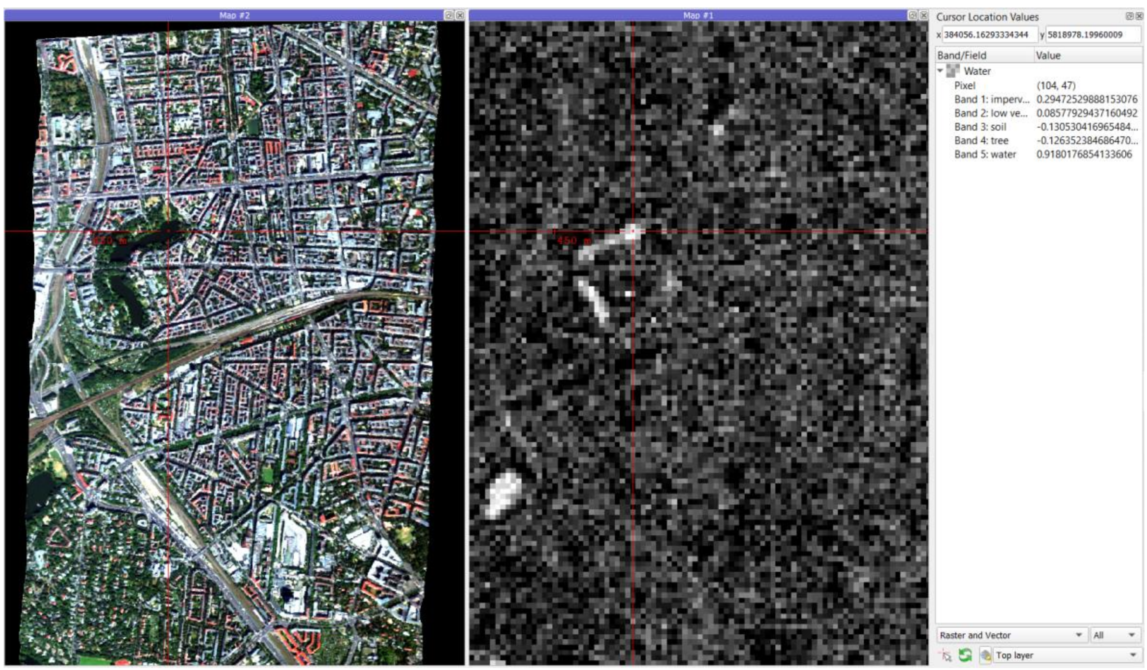

Figure 19. Water Class – Sample Pixel 2.

Tree Fractional Band (4)

For the Tree class (Figure 20), a high presence of Tree features should be observed in the left zone of the study area, based on the fractional map (Figure 20 - Right). This can be confirmed with the High-Resolution Image (Figure 20 – Left), and it's a good indicator of class performance. Regarding the fractional values for each sample pixel (Figure 21 – 22), the most predominant feature was the Tree class, with values of 0.65 and 1.04. As for the Water class, the Tree performance was good.

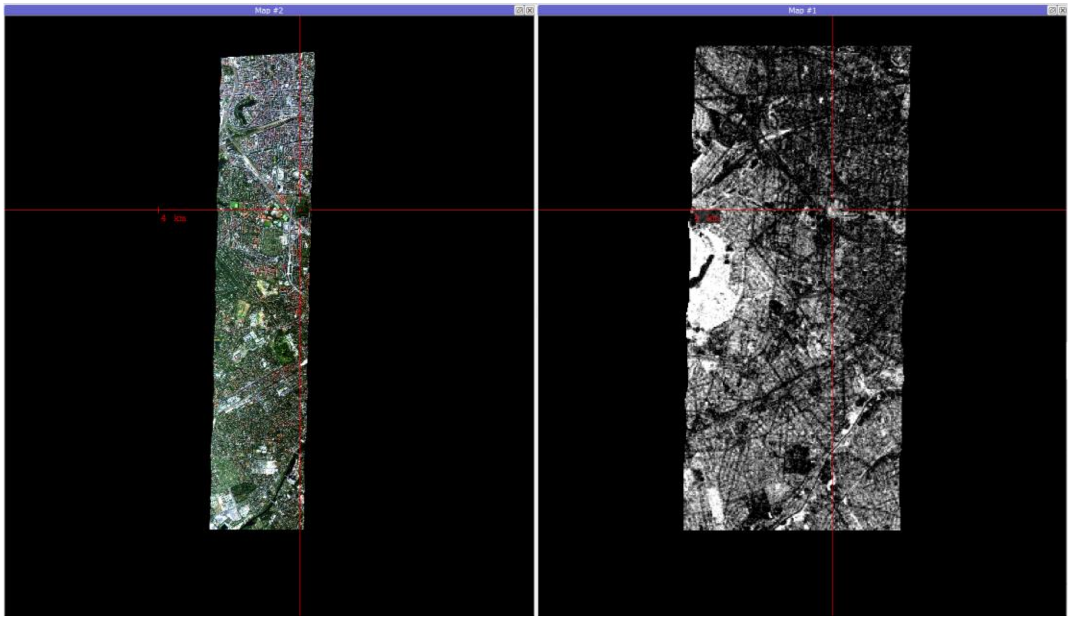

Figure 20. Tree Class - Fractional Map.

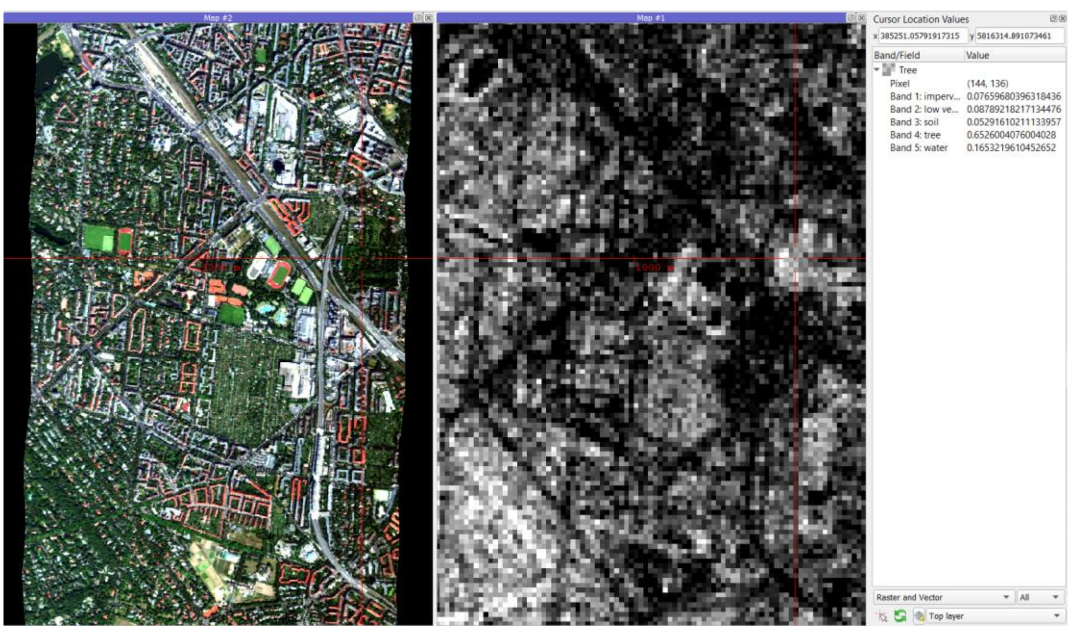

Figure 21. Tree Class – Sample Pixel 1.

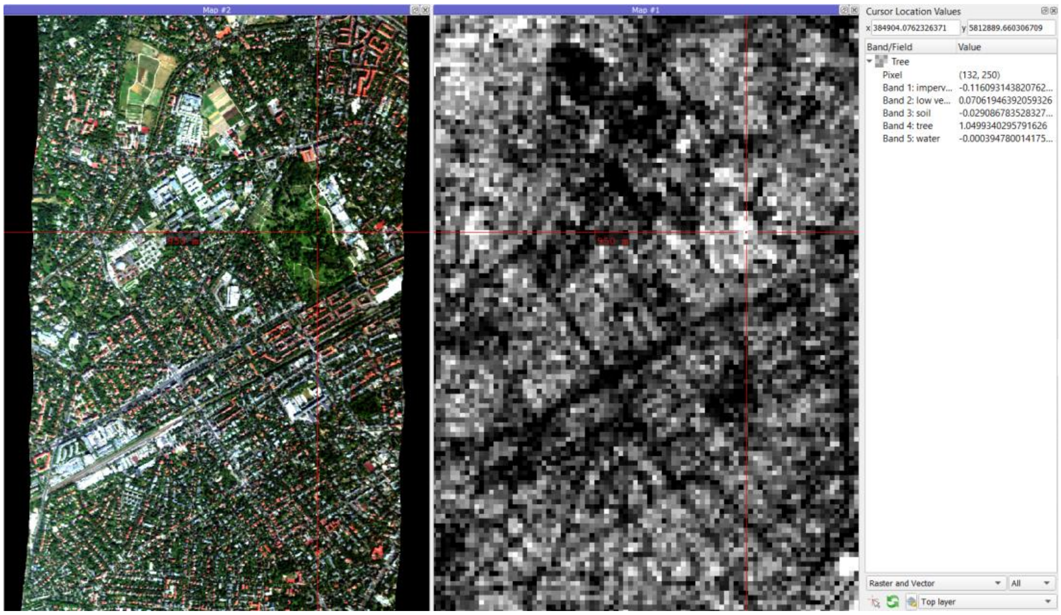

Figure 22. Tree Class – Sample Pixel 2.

Soil Fractional Band (3)

For the Soil class (Figure 23), small patches can be seen distributed along the study area. However, when comparing with the High-Resolution image (Figure 23 – Left), it can be evidenced that some pixels doesn't corresponds to soil but to impervious surfaces (Roofs). Regarding the fractional values (Figure 24 - 25), the Soil class performance was good, with 0.93 and 0.55 values. However, for the second sample, the low vegetation class was overestimated with a value of 0.38.

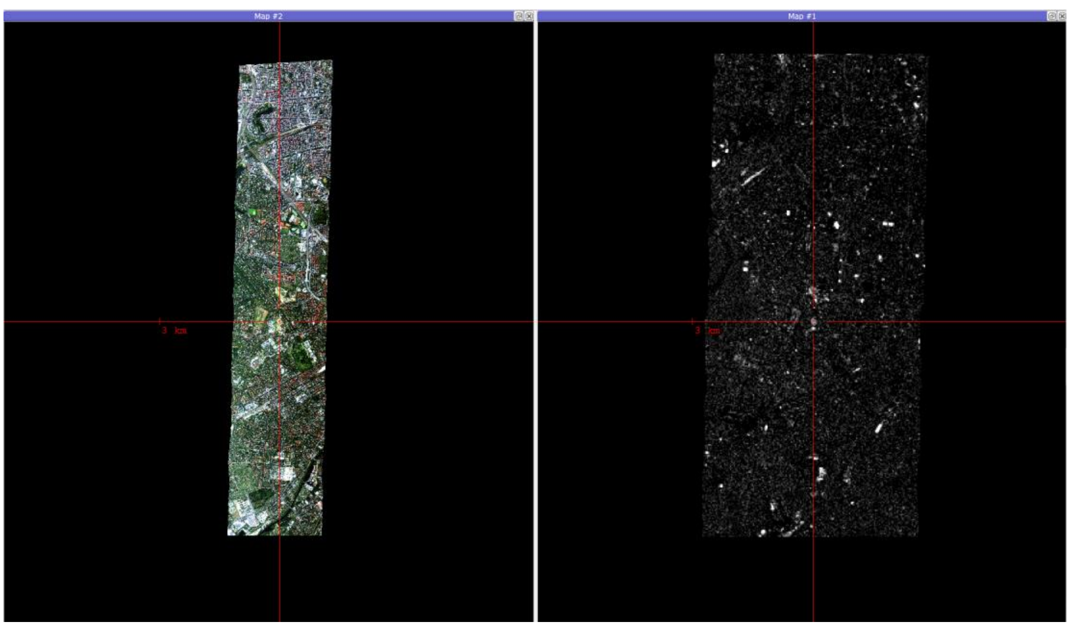

Figure 23. Soil Class - Fractional Map.

.

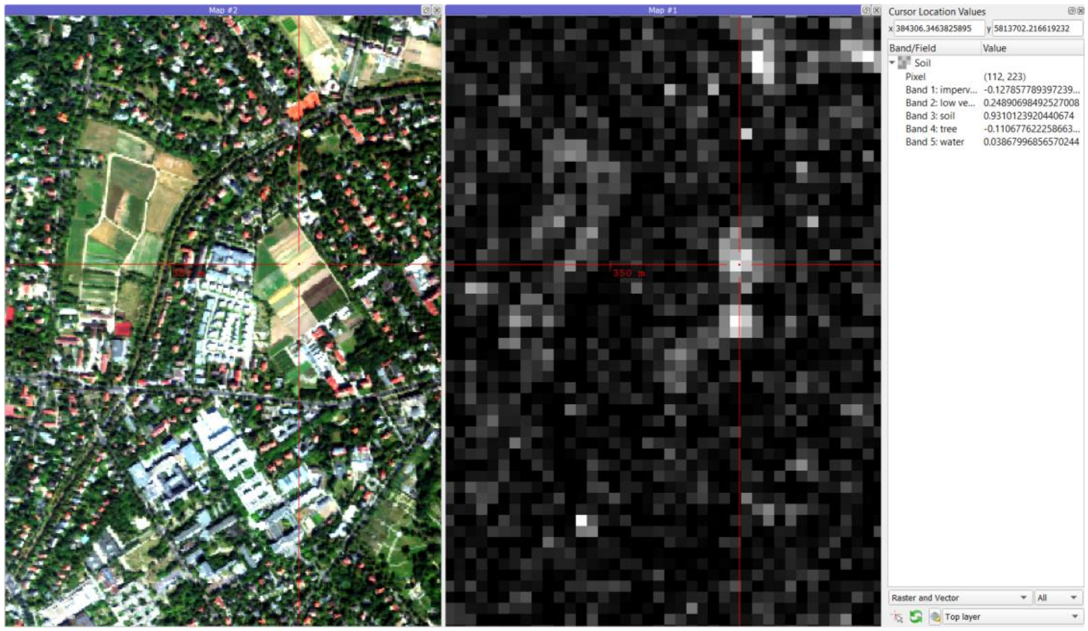

Figure 24. Soil Class – Sample Pixel 1.

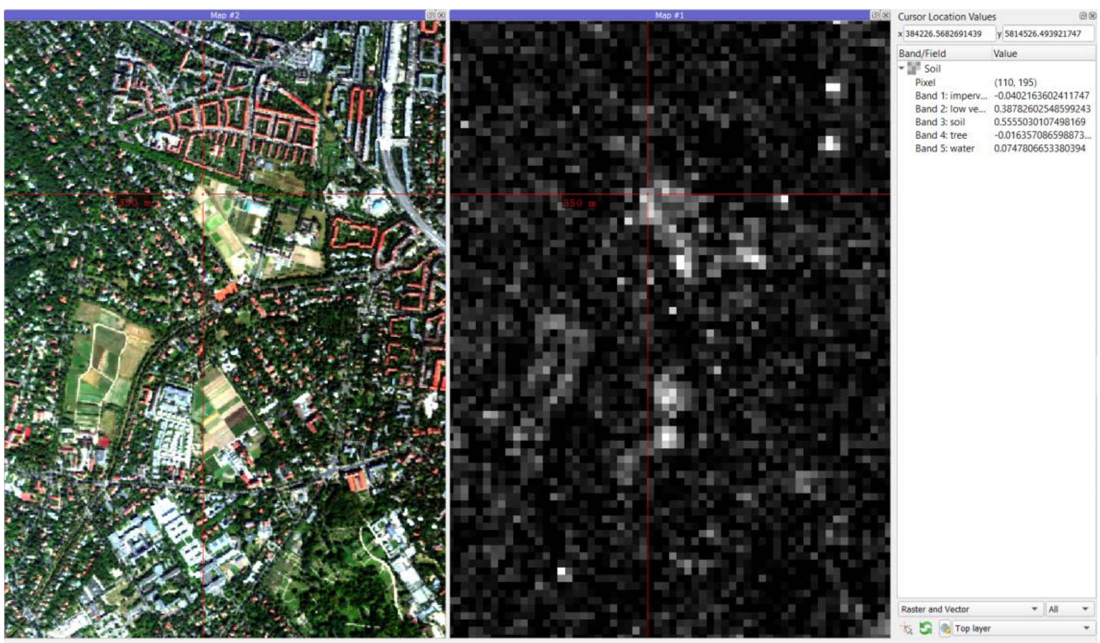

Figure 25. Soil Class – Sample Pixel 2.

Low Vegetation Fractional Band (2)

For the Low Vegetation class (Figure 26), it can be observed that it is distributed mainly through the suburban areas, this can be confirmed using the related High-Resolution image (Figure 23 – Left). Regarding the fractional values for each sample pixel (Figure 27 – 28), the most predominant class is effectively Low Vegetation, with values of 0.97 and 0.67.

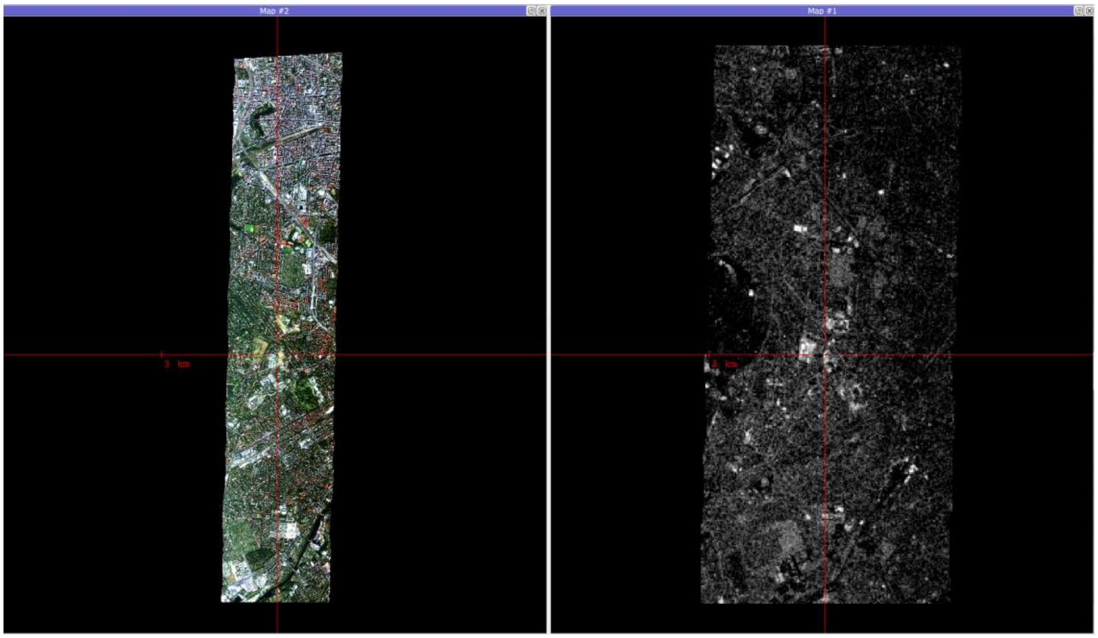

Figure 26. Low Vegetation Class - Fractional Map.

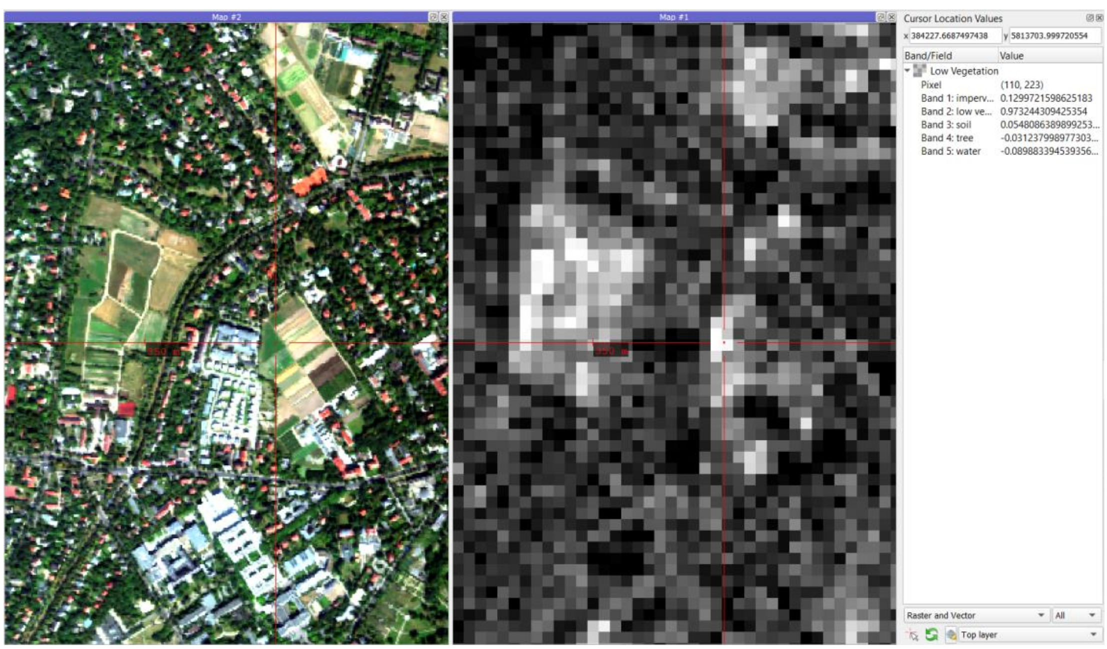

Figure 27. Low Vegetation Class – Sample Pixel 1.

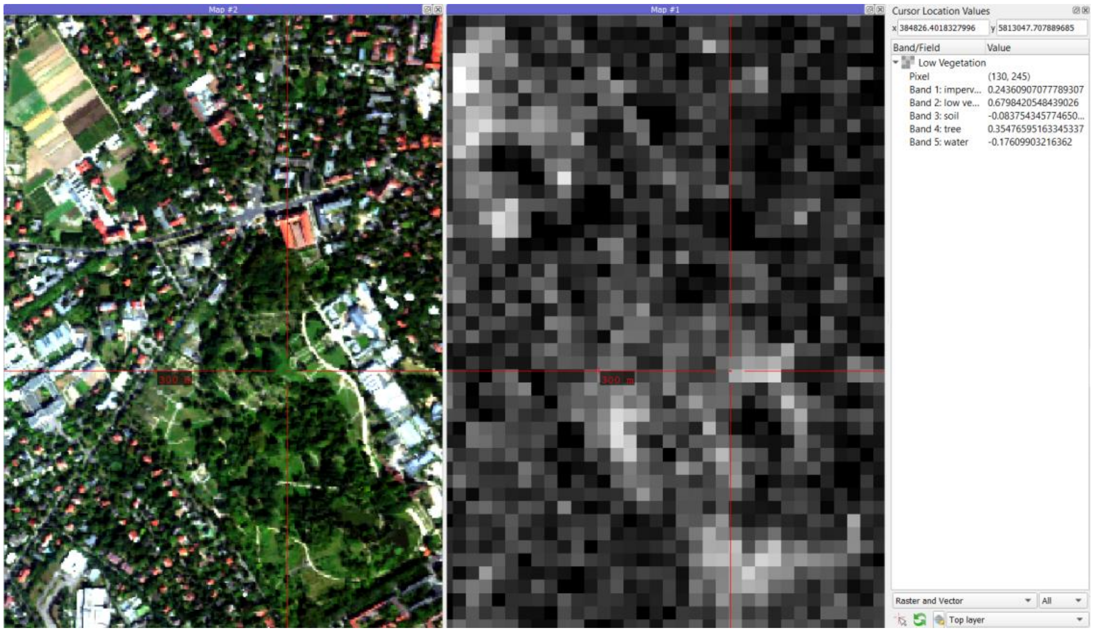

Figure 28. Low Vegetation Class – Sample Pixel 2.

Impervious Fractional Band (1)

Finally, the Impervious class (Figure 29) is distributed along all the study area. When comparing the fractional map with the High-Resolution image (Figure 29 – Left), it can observe that the features correspond to this class. Moreover, using the fractional values, this class evidence a good performance, as for both pixel samples (Figure 30 - 31) the predominant class is the Impervious one, with values of 0.86 and 1.00.

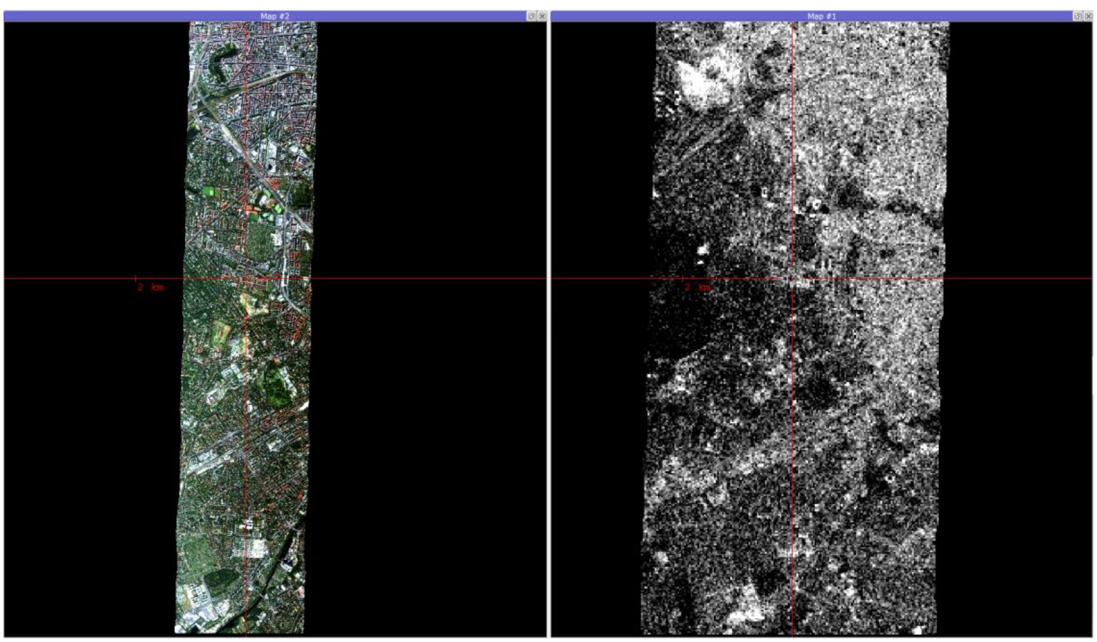

Figure 29. Impervious - Fractional Map

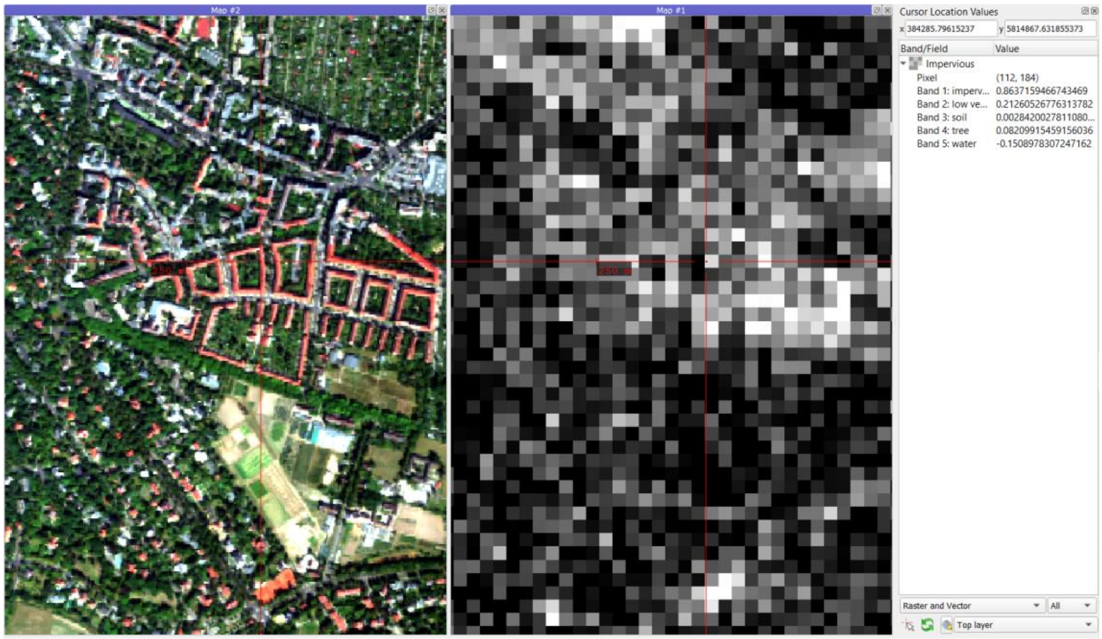

Figure 30. Impervious Class – Sample Pixel 1.

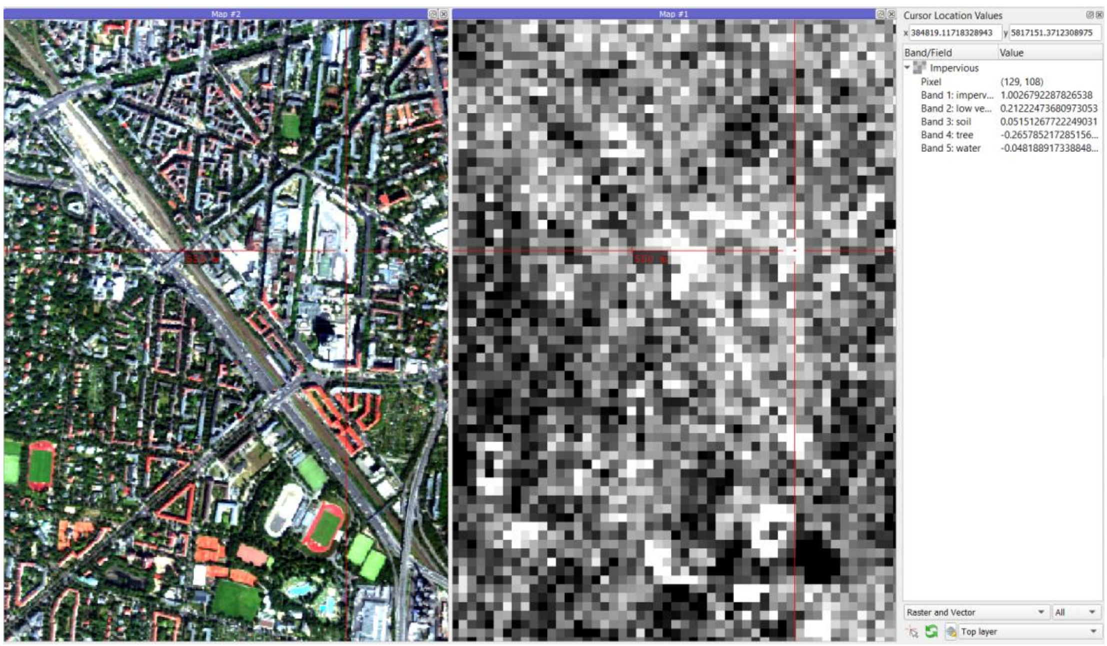

Figure 31. Impervious Class – Sample Pixel 2.

5. Conclusions

- The resulting Fraction layer obtained from the EnMAP "Regression-based Unmixing" approach, provides accurate discrimination (in a subpixel level) of the sampled classes. Good performance can be evidenced not only with visual comparisons but with coherent fraction values.
- High Resolution and Hyperspectral datasets can be used together to support advanced imagery analyses that require a high level of detail and multiple spectral bands.

6. References

EnMAP (February 5, 2019). Regression-based unmixing of urban land cover. Retrieved November 21, 2022, from https://enmap-box.readthedocs.io/en/latest/usr_section/application_tutorials/urban_unmixing/tutorial.html

European Space Agency (May 28, 2012). EnMAP. Retrieved November 21, 2022, from https://www.eoportal.org/satellite-missions/enmap#enmap-product-generation

Seos (n.d). Introduction to Remote Sensing. November 21, 2022, from https://seos-project.eu/remotesensing/remotesensing-c01-p06.html#:~:text=The%20spectral%20reflectance%20curve%20of%20bare%20soil%20is%20considerably%20less,observed%20in%20vegetation%20reflectance%20spectra

Twente University (n.d). Spectral reflectance curves. Retrieved November 21, 2022, from https://ltb.itc.utwente.nl/498/concept/81713